Two-Line Spatial Reflection Method for Measuring Wood Grain Direction

Qi (Patrick) Pan
Gary S. Schajer

Abstract

Wood grain direction is a three-dimensional quantity that is defined by its angles within and into the plane of the measured surface. These are respectively called the surface and dive angles. An interesting method to measure these angles involves measuring the spatial reflection from the wood surface when illuminated by concentrated light. The cellular shape of the wood microstructure causes the light reflection to be greatest perpendicular to the wood grain. This effect allows the surface and dive angles to be determined by analyzing the spatial variation of the reflected light. The conventional method for doing this involves sampling the reflection intensities around a circle above the wood surface. However, this method is effective only for small dive angles. A new method is described here where light reflection intensity variation is measured along two parallel lines on either side of the illuminated area. It is able to measure the ranges of surface and dive angles of interest in strength grading applications. A laboratory device for making the required spatial reflection measurements is described and experimental results are presented.

Wood is a natural material that has large variations in grain structure, mostly due to the presence of knots and spiral grain. The resulting variations in wood grain (fiber) direction strongly affect the strength of the wood; even a small deviation in grain direction significantly weakens the lumber. For example, a 15° deviation of the grain direction can approximately halve the lumber strength (Kretschmann 2010). This effect is recognized explicitly for strength-sensitive applications; in the case of wooden ladder construction, ANSI Standard A14.1 (American National Standards Institute 2007) specifies a maximum allowable slope of grain for the wood to be 1:12, which corresponds to a grain angle of 4.8°. Thus, for general strength grade wood quality control, it is important to be able to measure wood grain direction effectively and reliably, particularly over the lower to middle angle ranges.

In sawmills, lumber grain direction has traditionally been determined by visual inspection by skilled graders (Canadian Wood Council 2016). However, it is a time-consuming process with low consistency because of the high degree of personal judgment required.

There are several modern techniques of measuring wood grain direction, each with its particular features. The longitudinal arrangement of wood fibers causes lumber to be anisotropic in various physical properties. For example, the dielectric anisotropy of wood can be exploited to allow noncontact measurements of surface angle in real time using radio frequency (McLauchlan et al. 1973) and microwave (Schajer and Orhan 2006) measurements. An X-ray diffractometry approach has also been used to measure the grain angle, but the samples require very delicate preparation (Buksnowitz et al. 2008).

Laser scanning provides an alternative practical method for measuring wood grain angle. Most laser-scanning techniques are based on the ellipse method. When a wood surface is illuminated by a concentrated light source such as a laser, the light tends to spread along the wood fibers at the surface to form an elliptical illuminated spot (Zhou and Shen 2003, Faria et al. 2008, Brannstrom et al. 2008, Astrand 2011). The same effect can be obtained by transillumination imaging (Nieminen et al. 2013), where a near-infrared laser light source illuminates a wood sample from behind and the light transmitted through the sample is captured by a camera at the front of the sample. Taking the concept of long-wavelength illumination a step further, the ellipse has been implemented to detect the presence of knots by locally heating the wood surface and measuring the response using a thermal camera (Daval et al. 2015). A limitation of the ellipse method is that it measures surface angle only. An attempt has been made also to infer the dive angle (Simonaho et al. 2004), but the measurement resolution is very low.

The authors are, respectively, Graduate Student and Professor, Dept. of Mechanical Engineering, Univ. of British Columbia, Vancouver, British Columbia, Canada (patrick.p8776@gmail.com, schajer@mech.ubc.ca [corresponding author]). Patrick Pan is the winner of the FPS 2017 Wood Award. This paper was received for publication in February 2018. Article no. 18-00004.

Forest Prod. J. 68(4):459–464.
doi:10.13073/FPJ-D-18-00004

In addition to the within-surface spreading of light due to the ellipse method when wood is illuminated by a concentrated light source, light also reflects from the wood surface to form a spatial pattern shaped by the wood grain direction. At the microscopic scale, wood material is composed of many parallel cylindrical cells (Core et al. 1979). When incident light strikes the surface of the cylindrical cells, the reflection preferentially fans out perpendicular to the grain (Matthews and Soest 1986). This is an example of a more general optical characteristic of many material surfaces where light reflects in a way that has a characteristic spatial distribution that is neither fully specular (mirrorlike) or fully diffuse. Mathematically, this effect is described by the bidirectional reflectance distribution function (Nicodemus 1965). Matthews and Soest (1986) developed a system that samples the reflected light around a circular path parallel to the wood surface to determine both the surface and the dive angles of the wood. An alternative measurement approach is to reverse the actions of the light source and sensor and instead rotate the light source around the wood sample and measure the reflected light normal to the wood surface (McGunnigle 2009). More recently, a digital camera has been used to measure the distribution of the reflected light (Schajer and Sutton 2016). The ability to measure both surface and dive angles is a particular feature of the light reflection method that distinguishes it from the previously mentioned wood grain angle measurement techniques that measure surface angle only.

A limitation of the method of making measurements around a circular path is that it can measure only smaller dive angles, typically $<5°$ (Schajer and Sutton 2016). This article describes a new approach to enable measurements of larger dive angles, thereby giving the technique a wider range of applicability.

Theory

When light impinges on a wood surface it partially reflects as a mixture of specular and diffuse light. The specular component is a mirrorlike reflection that travels at a single, sharply defined outgoing direction, whereas the diffuse component reflects out smoothly over a wide range of directions. The specular component is of particular interest here.

The cylindrical structure of wood causes the specular reflection from a concentrated illuminated spot of the surface to fan out within the normal plane of the cylinders, as shown in Figure 1. If the fiber direction is parallel to the wood surface, as in Figure 1a, the fan of specularly reflected light is planar. If a flat plane is imagined parallel to the wood surface, the fan of light would intersect it to form a straight line. If, however, the fiber direction dives into the wood surface, as in Figure 1b, then the fan of specularly reflected light forms a slightly conical shape and the intersection with the plane becomes curved. Figure 1 illustrates the response of the specular component of the reflected light. The diffuse component combines with the specular component to give a more spread-out response.

The established way to identify the wood surface and dive angles from the reflected light pattern is the circle method (Matthews and Soest 1986). The reflected light intensity is measured by sensors arranged around a circular path on the measurement plane shown in Figure 2. The circle has radius R and the measurement plane is at distance h from the wood surface. In Figure 2a, where both surface and dive angles are zero, the circle intersects the reflected light pattern symmetrically, so a graph of measured light intensity versus circumferential angle will show two peaks at $\phi_1 = 90°$ and $\phi_2 = 270°$. If the surface grain angle α rotates, then the reflected light pattern and the positions of the two peaks will change correspondingly. If, instead, the dive angle δ changes, the reflected light pattern moves sideways, causing the positions of the two peaks to move either closer together or farther apart. From the geometry of the specular reflection pattern it may be shown that the surface and dive angles may be computed from the positions of the two light intensity peaks ϕ_1 and ϕ_2 using (Matthews and Soest 1986):

$$\text{Surface angle:}\quad \alpha = \frac{\phi_1 + \phi_2}{2} - 90^{\circ} \tag{1}$$

$$\text{Dive angle:}\quad \tan\delta = \tan\frac{\theta}{2}\cos\frac{\phi_1 - \phi_2}{2} = \tan\frac{\theta}{2}\cos\phi \tag{2}$$

where

$$\tan\theta = \frac{R}{h} \tag{3}$$

The subtraction between ϕ_1 and ϕ_2 can also be expressed as ϕ, as marked in Figure 2c.

A difficulty occurs with increasing dive angle. As the area of reflected light moves sideways, the line of maximum intensity becomes more tangential to the circular path of light sensors. This causes the two measured light intensity peaks to become closer together and less distinct, as shown in Figure 2d. This indistinctness impedes reliable determination of ϕ_1 and ϕ_2, thus preventing practical evaluation of large dive angles.

The ''two-line'' method is introduced here to keep the measurement lines more perpendicular to the line of maximum light intensity and thereby avoid the tangential response of the circle method.

In the proposed method, measurements are made along parallel lines at distance g at either side of the illuminated spot, as shown in Figure 3. The measurement plane remains at distance h above the wood surface. The axial distances of the light intensity peaks from the center line, y_1 and y_2, are measured, from which the corresponding angles ϕ_{11} and ϕ_{12} (at radius R_1) and ϕ_{21} and ϕ_{22} (at radius R_2) can be determined. The surface and dive angles can then be evaluated using Equation 1 for each of the two circles R_1 and R_2 in Figure 3.

Experimental Apparatus

Figure 4 schematically illustrates the apparatus used for the wood grain angle measurements reported here. Each wood specimen was mounted on an optical table and illuminated by a laser diode from a 5-mW 660-nm laser pointer with a 1.5-mm-diameter spot size. So that it would not obstruct the viewing area adjacent to the wood surface, the laser diode was mounted remotely at the side of the wood specimen. The light beam was reflected onto the wood surface by a 45° mirror, as shown in the diagram. This mirror was made very small, <2 mm across, so as to minimize its obstruction of the viewing area. In addition, it was mounted on a glass plate so that its mechanical support would not cause any further optical obstruction. Initial setup was done by first aligning the camera image center perpendicular to the target spot on the specimen surface.

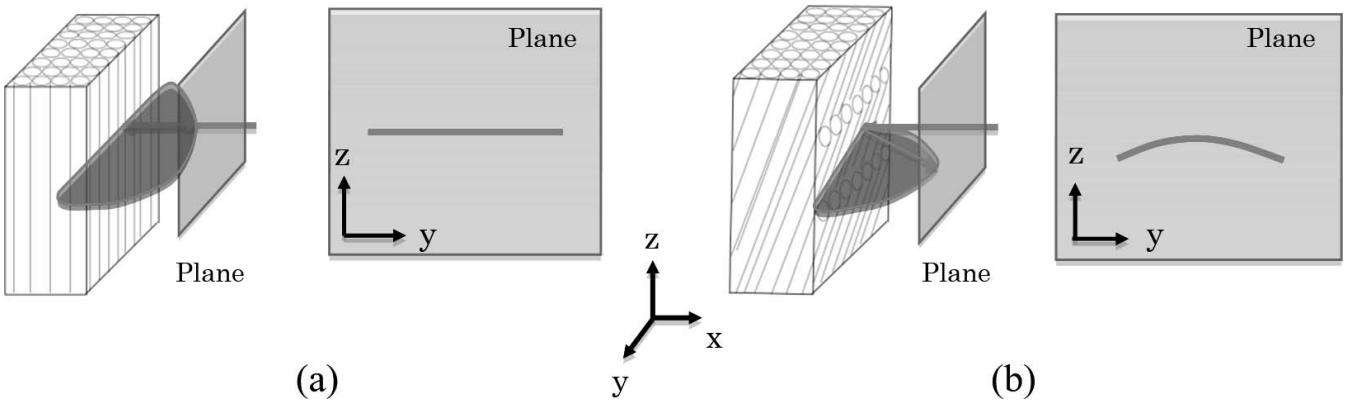

Figure 1.—Specular reflection from a cylindrical wood cell: (a) cell parallel to wood surface and (b) cell diving into wood surface.

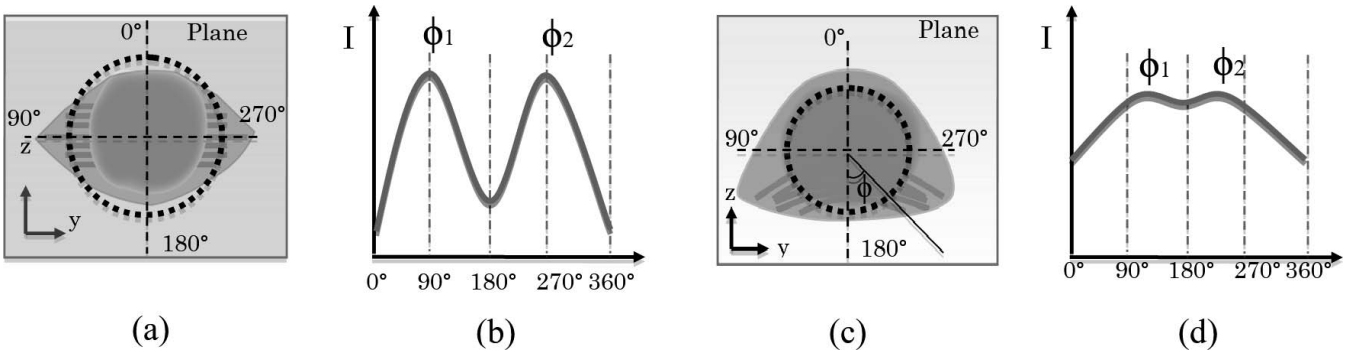

Figure 2.—Wood spatial reflection measurement around a circle: (a) zero dive angle, (b) circumferential variation of light intensity, (c) large dive angle, and (d) circumferential variation of light intensity.

Then the small 45° mirror was put in place so that it symmetrically covered the target spot in the camera image. Finally, the laser illumination was adjusted so that the illuminated spot on the wood surface was in the correct position and was fully shadowed by the small mirror so as not to appear directly in the camera image.

Light reflection measurements were made using an OPT101 photodiode (Texas Instruments, Dallas, Texas, USA) connected to a custom-made signal conditioner. The photodiode was mounted to a three-axis motorized table so that it could move in a controlled manner within the space adjacent to the wood surface. The photodiode could then be moved systematically to measure a detailed map of the surface reflection pattern radiating from the illuminated spot on the wood specimen.

Three sample wood specimens, 50 by 15 by 5 mm, were prepared so that they all had parallel surface grain directions, $\alpha = 0°$, but different dive angles, $\delta = 0°$, 6°, and 10°, as observed microscopically. They are all of Englemann spruce (*Picea engelmannii*), a prominent commercial species in the local wood industry. This range of grain angles was chosen to focus on the range of interest when assessing wood for strength grade applications.

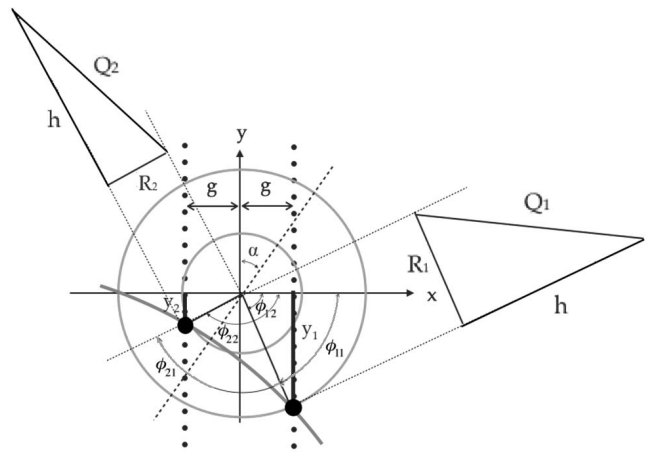

Figure 3.—Geometry of the two-line method.

Experimental Measurements

Figure 5 shows the spatial reflection map measured by scanning the sensor at 1-mm intervals, column by column, to form an image. The smoothly varying light intensity indicates that the reflected light is a mixture of specular and diffuse components. The figure shows the measured data, without any additional mathematical smoothing. As the dive angle of the specimen increases from 0° to 10°, the brightest part of the reflection displaces sideways.

The motorized table was programmed to move the sensor in 72, 5° steps around a circle at radius $R_1 = 15$ mm at a distance $h = 30$ mm above each specimen surface. Figure 6 shows the measured reflected light intensity curves.

For the first specimen with 0° dive angle, the two peaks in the intensity curve in Figure 6a are distinct, giving a well-defined result $\delta = 0.6°$. For the second specimen with 6° dive

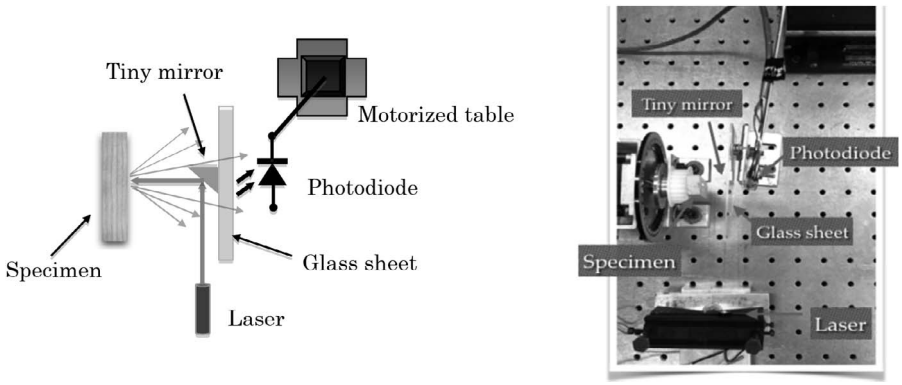

Figure 4.—Experimental apparatus: (a) schematic diagram and (b) photographic view.

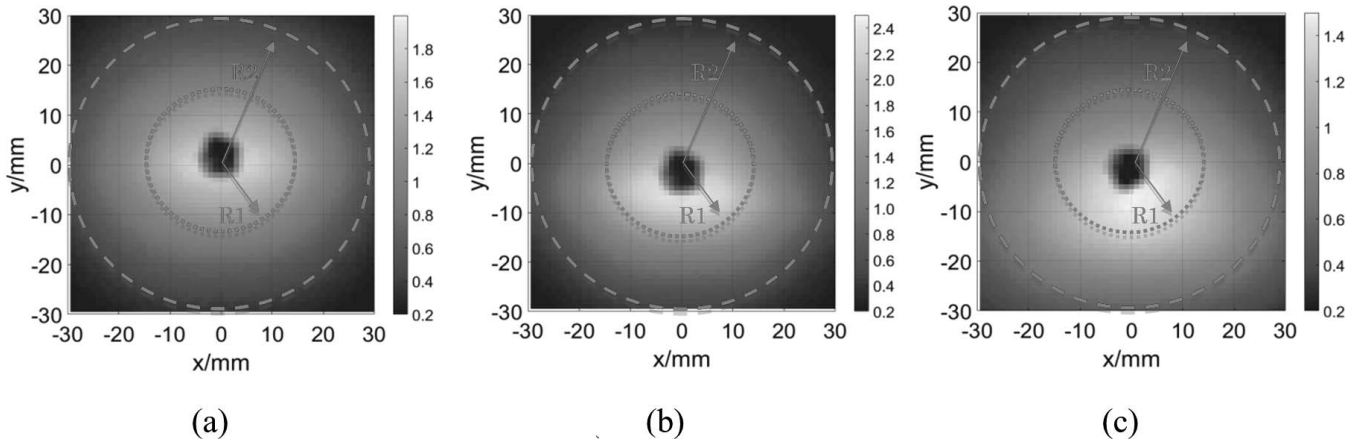

Figure 5.—Measured reflection intensity maps. $R_1 = 15$ *mm,* $h = 30$ *mm. Spatial resolution = 1 mm. (a) Dive angle* $\delta = 0°$*, (b) dive angle* $\delta = 6°$*, and (c) dive angle* $\delta = 10°$*.*

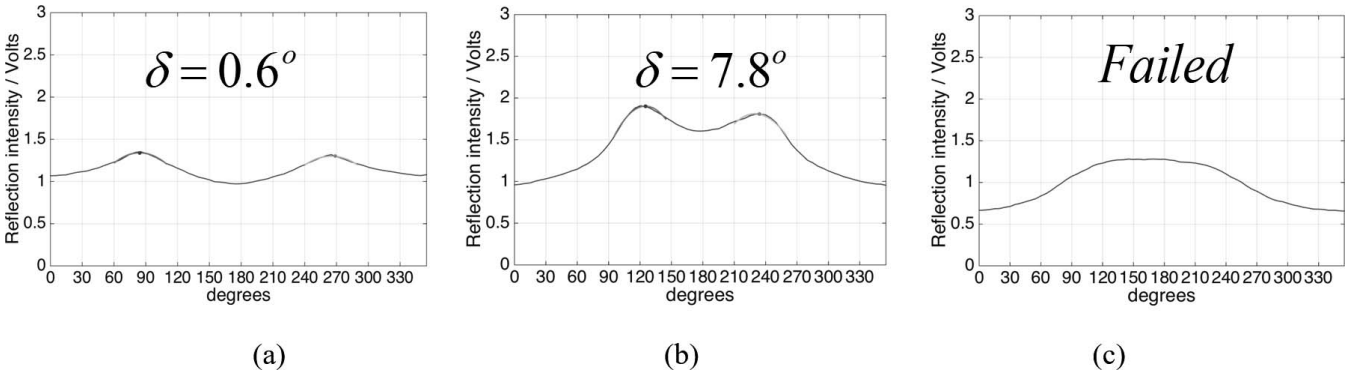

Figure 6.—Reflection intensity measured around a circle with $R_1 = 15$ *mm and* $h = 30$ *mm. (a) Dive angle* $\delta = 0°$*, (b) dive angle* $\delta = 6°$*, and (c) dive angle* $\delta = 10°$*.*

angle, the two light intensity peaks in Figure 6b move closer and become a little less distinct, but the measurement was still successful to give $\delta = 7.8°$. However, for the third specimen with 10° dive angle, the light intensity peaks in Figure 6c have moved so much together that they have merged into one. Thus, it is not possible to identify individual angles ϕ_1 and ϕ_2, causing the measurement to fail. The reason for the problem can be seen in Figure 5c, where the maximum reflection peak has moved to become tangential to the R_1 circle. A larger circle will ameliorate the tangential measurement problem, but the received light intensity will become reduced at the greater distance and the specular peaks less distinct.

The large diffuse component in the reflected light is the major cause of the specular peaks becoming indistinct, thereby creating the difficulties encountered. An effective way was developed to separate the diffuse effect from the specular effect by scaling the data to flatten out the diffuse reflection component. The various points within the reflection intensity maps in Figure 5 have differing distances

Q from the illuminated spot on the wood surface (see Fig. 3), causing the measured light intensity to vary according to the inverse square law. This effect can be compensated for by multiplying the measured light intensities by $(Q/h)^2$. An additional effect occurs because the light reflection from a diffuse surface varies with direction according to Lambert's law, which here requires an additional compensation factor Q/h. Combining these gives a required compensation factor $(Q/h)^3$. The light sensor used here also had some directional dependence. After some tests using plane diffuse surfaces, it was found that the flattest response was achieved from the sensor measurements by scaling by $(Q/h)^{2.5}$.

Figure 7 shows the scaled reflection intensity maps for the measurements shown in Figure 5. It can be seen that the scaling is very effective at flattening the diffuse reflection component and thereby making the specular component more visible against that flat background. The specular component also extends sideways to a much greater extent, thus making it easier to identify. These effects greatly add to the quality of the feature extraction.

The distance Q of each measurement point to the illuminated spot on the wood surface is constant around a circular path. The circle method light intensity profile shown in Figure 6 is scaled vertically by a uniform factor because all points around the circle have the same distance and inclination angle to the illuminated spot. Because their underlying shapes do not change, the peak positions remain the same. Thus the previously computed dive angles $\delta =$ 0.6°, 7.8°, and ''failed'' remain unchanged.

Figure 8 shows the parallel arrangement of measurement lines used by the two-line method. These lines are much more perpendicular to the specular reflection line than the previous circle, so should give more sharply defined peaks and thus better results.

Figure 9 shows the scaled reflection intensity curves corresponding to $g_1 = 15$ mm in Figure 8. The dive angles computed from them are $\delta = 0.2°$, 6.7°, and 9.9°, which compare very well with the microscopically measured values 0°, 6°, and 10°. The profile for the 10° specimen shows a much flatter curve, indicating that the associated grain angle result will be more susceptible to measurement noise. The more perpendicular orientation of the measurement line through the reflected light field shown in Figure 8 maximizes the opportunity to detect the local maximum. In contrast, the circle-method measurement line is parallel to the reflected light field in Figure 7 and so has much reduced

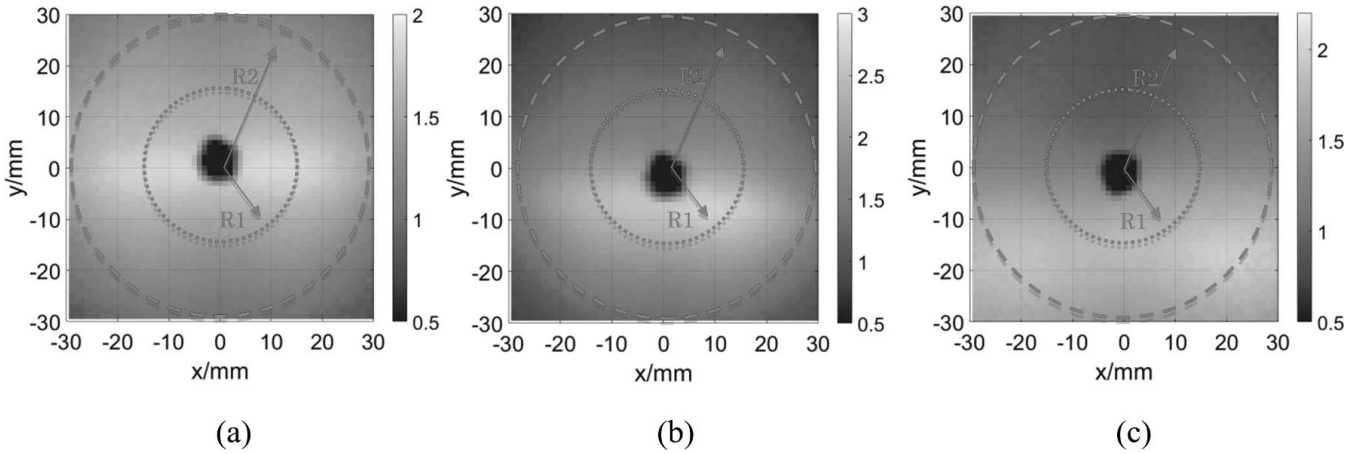

Figure 7.—Reflection intensity maps scaled using $(Q/h)^{2.5}$. $R_1 = 15$ *mm,* $h = 30$ *mm. (a) Dive angle* $\delta = 0°$*, (b) dive angle* $\delta = 6°$*, and (c) dive angle* $\delta = 10°$.

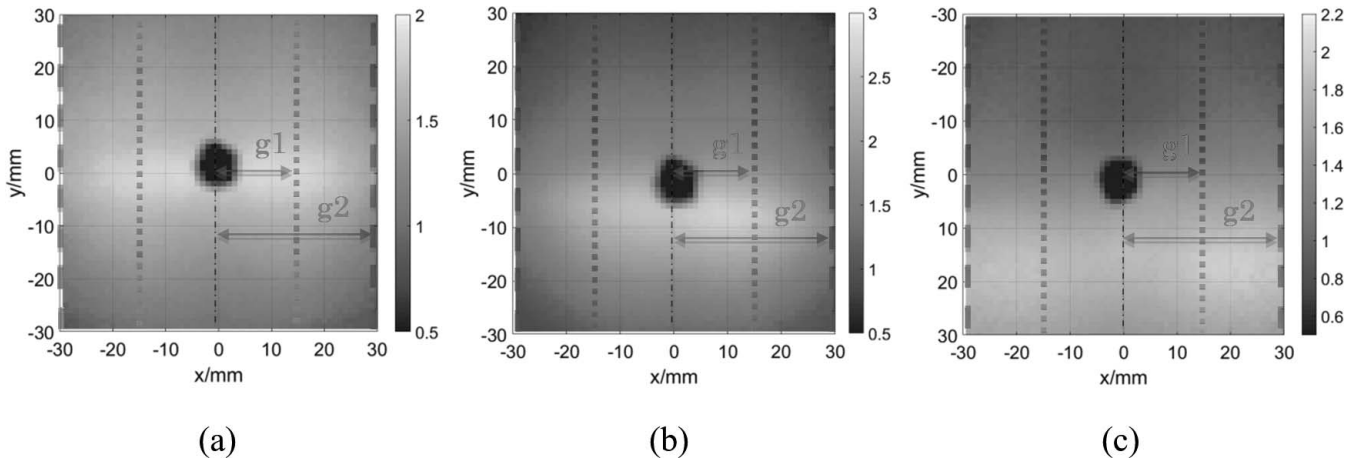

Figure 8.—Reflection intensity maps scaled using $(Q/h)^{2.5}$. $g_1 = 15$ *mm,* $h = 30$ *mm. (a) Dive angle* $\delta = 0°$*, (b) dive angle* $\delta = 6°$*, and (c) dive angle* $\delta = 10°$.

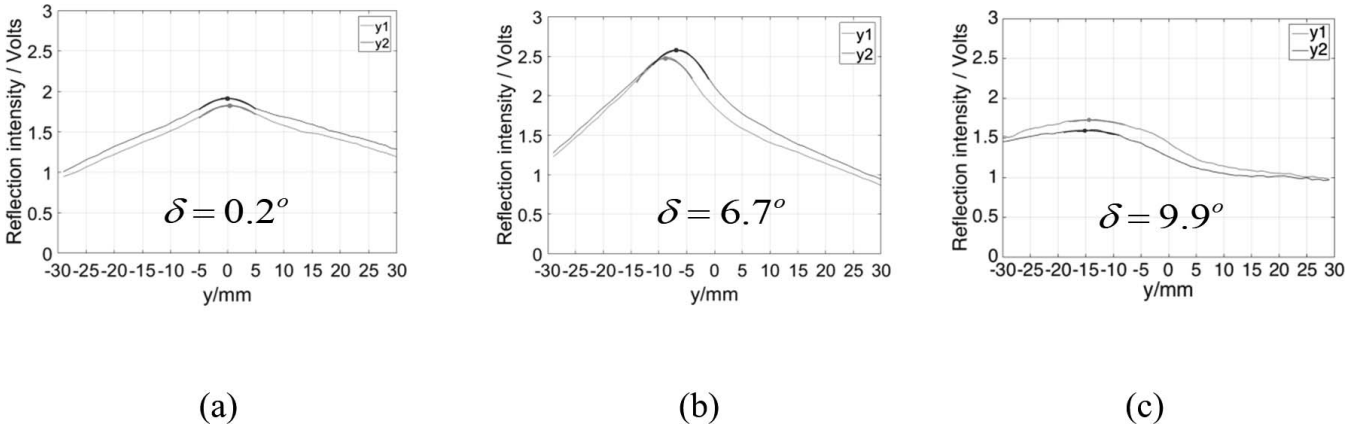

Figure 9.—Scaled reflection intensity curves along parallel lines. $g_2 = 30$ *mm,* $h = 30$ *mm. (a) Dive angle* $\delta = 0°$*, (b) dive angle* $\delta = 6°$*, and (c) dive angle* $\delta = 10°$.

opportunity to find a local maximum, thereby causing failure in this case. These results demonstrate the improved capability of the two-line method to measure dive angle.

Conclusions

The light reflection method developed here provides an important method for measuring wood grain orientation because it is capable of measuring both surface and diving grain angles. The established approach of measuring the reflected light around a circle concentric with the illumination point was found to have limited capability to measure diving grain angles beyond about 6°. This limitation occurs because larger dive angles cause the specular component of the wood surface reflection to become increasingly tangential to the measurement circle, thereby inhibiting the ability of the measurement method to distinguish local light intensity peaks. The proposed method replaces the previous measurement circle with two parallel lines. These remain more perpendicular to the specular component of the wood surface reflection over a much greater range of dive angles.

An important additional step to make the specular reflective light component more distinctive and easier to locate is to flatten the diffuse reflective light component by scaling the measured reflected light by factors that compensate for the operations of the inverse square law and Lambert's law. This scaling is very effective and enables the superimposed specular light component to appear clearly as a distinctive line. Overall, this proof-of-concept study has demonstrated that the proposed two-line method can be effective at measuring both surface and dive angles in wood.

Acknowledgments

This work was financially supported by grants from Hermary Optoelectronics, Inc. and from the Natural Science and Engineering Research Council of Canada (NSERC). The authors also sincerely thank Darren Sutton for his many helpful comments and suggestions

Literature Cited

American National Standards Institute (ANSI). 2007. American national standards for ladders—Wood safety requirements. Standard A14.1. ANSI, Washington, D.C.

Astrand, E. 2011. Building a high-performance camera for wood inspection. *EETimes*. http://www.eetimes.com/document.asp?doc_id=1279213. Accessed December 11, 2016.

Brannstrom, M., J. Manninen, and J. Oja. 2008. Predicting the strength of sawn wood by tracheid laser scattering. *BioResources* 3(2):437–451.

Buksnowitz, C., U. Muller, R. Evans, A. Teischinger, and M. Grabner. 2008. The potential of SilviScan's X-ray diffractometry method for the rapid assessment of spiral grain in softwood, evaluated by goniometric measurements. *Wood Sci. Technol*. 42(2):95–102.

Canadian Wood Council. 2016. Grades. http://cwc.ca/wood-products/lumber/visually-graded/grades/. Accessed December 11, 2016.

Core, H. A., W. A. Côté, and A. C. Day. 1979. Wood Structure and Identification. Syracuse University Press, Syracuse, New York.

Daval, V., G. Pot, M. Belkacemi, F. Meriaudeau, and R. Collet. 2015. Automatic measurement of wood fiber orientation and knot detection using an optical system based on heating conduction. *Opt. Soc. Am*. 23(26):33529–33539.

Faria, R., R. Braga, Jr., A. Neto, N. Trindade, F. Mori, and G. Horgan. 2008. Reliability of wood grain orientation measurement using laser illumination. *Biosyst. Eng*. 100(4):479–483.

Kretschmann, D. 2010. Mechanical properties of wood, chap. 5. *In:* Wood Handbook, Wood as an Engineering Material. FPL-GTR-190. USDA Forest Products Laboratory, Madison, Wisconsin.

Matthews, P. C. and J. F. Soest, 1986. Method for determining localized fiber angle in a three dimensional fibrous material. US patent 4606645. US Patent and Trademark Office, Washington, D.C.

McGunnigle, G. 2009. Estimating fibre orientation in spruce using lighting direction. *IET Comput. Vis*. 3(3):143–158.

McLauchlan, T. A., J. A. Norton, and D. J. Kusec. 1973. Slope of grain indicator. *Forest Prod. J*. 23(5):50–55.

Nicodemus, F. 1965. Directional reflectance and emissivity of an opaque surface. *Appl. Opt*. 4(7):767–775.

Nieminen, S., J. Heikkinen, and J. Raty. 2013. Laser transillumination imaging for determining wood defects and grain angle. *Meas. Sci. Technol*. 24(12):125401.

Schajer, G. S. and F. B. Orhan, 2006. Measurement of wood grain angle, moisture content and density using microwaves. *Holz Roh- Werkst*. 64(6):483–490.

Schajer, G. S. and D. B. Sutton. 2016. Identification of 3D wood grain angle by directional reflection measurement. *Wood Mater. Sci. Eng*. 11(3):170–175.

Simonaho, S.-P., J. Palviainen, Y. Tolonen, and R. Silvennoinen. 2004. Determination of wood grain direction from laser light scattering pattern. *Opt. Lasers Eng*. 41(1):95–103.

Zhou, J. and J. Shen. 2003. Ellipse detection and phase demodulation for wood grain orientation measurement based on the tracheid effect. *Opt. Lasers Eng*. 39(1):73–89.